

## From ballistic motion to localization: a phase space analysis

André Wobst, Gert-Ludwig Ingold, Peter Hänggi, Dietmar Weinmann

### Angaben zur Veröffentlichung / Publication details:

Wobst, André, Gert-Ludwig Ingold, Peter Hänggi, and Dietmar Weinmann. 2002. "From ballistic motion to localization: a phase space analysis." *The European Physical Journal B: Condensed Matter and Complex Systems* 27 (1): 11-14. <https://doi.org/10.1140/epjb/e20020125>.

### Nutzungsbedingungen / Terms of use:

licgercopyright

Dieses Dokument wird unter folgenden Bedingungen zur Verfügung gestellt: / This document is made available under these conditions:

**Deutsches Urheberrecht**

Weitere Informationen finden Sie unter: / For more information see:

<https://www.uni-augsburg.de/de/organisation/bibliothek/publizieren-zitieren-archivieren/publiz/>



# From ballistic motion to localization: a phase space analysis

A. Wobst<sup>1</sup>, G.-L. Ingold<sup>1,a</sup>, P. Hänggi<sup>1</sup>, and D. Weinmann<sup>2</sup>

<sup>1</sup> Institut für Physik, Universität Augsburg, Universitätsstrasse 1, 86135 Augsburg, Germany

<sup>2</sup> Institut de Physique et Chimie des Matériaux de Strasbourg<sup>b</sup>, 23 rue du Loess, 67037 Strasbourg Cedex, France

**Abstract.** We introduce phase space concepts to describe quantum states in a disordered system. The merits of an inverse participation ratio defined on the basis of the Husimi function are demonstrated by a numerical study of the Anderson model in one, two, and three dimensions. Contrary to the inverse participation ratios in real and momentum space, the corresponding phase space quantity allows for a distinction between the ballistic, diffusive, and localized regimes on a unique footing and provides valuable insight into the structure of the eigenstates.

The behavior of a quantum particle in a disorder potential depends significantly on the disorder strength. If the mean free path exceeds the system size, one may think of plane waves characterized by a fixed momentum which are scattered by the weak random potential. On the other hand, sufficiently strong disorder leads to exponentially localized states in real space. Then a wide range of momenta is needed to construct these states. A description for arbitrary disorder strength thus requires to adequately take into account real space as well as momentum space properties. It is therefore appropriate to treat the system in phase space. Moreover, phase space quantities have recently been measured in experiments on light scattering from disordered media [1]. Hence, in the following we will develop a phase space approach to disordered systems.

Signatures of the different regimes can already be found in the energy spectrum. While for weak and strong disorder energy levels can almost be degenerate, level repulsion occurs in an intermediate regime. Making use of random matrix theory the chaotic nature can be verified and related to diffusive motion. However, such considerations cover only statistical properties of the spectrum and do not give information about the structure of individual states.

A popular way to investigate the properties of single states is the calculation of their inverse participation ratio (IPR). In real space this quantity has frequently been employed [2] to measure the size of the localization domain of quantum states in the localized regime and to characterize the Anderson transition [3,4]. Furthermore,

an analysis based on the IPR has been performed for the eigenmodes of disordered microwave cavities [5]. However, the real space IPR is not very sensitive to changes in extended wave functions when going from the ballistic to the diffusive regime. In order to obtain a meaningful description of the structure of quantum states for all regimes on a unique footing, we generalize the concept of the IPR to phase space.

The Anderson model of disordered solids [6] has been the subject of extensive investigations over the last decades [7]. A numerical study of this model in one, two, and three dimensions and comparison with energy level statistics will demonstrate the virtues of our approach. The IPR in phase space enables us to individually characterize eigenstates and to identify ballistic, diffusive, and localized regimes. In particular, the results in one dimension will significantly differ from those in higher dimensions, which can be attributed to the absence of a diffusive regime.

We start by introducing the relevant phase space concepts. At this point there is no need to specify the details of the disordered system except that we will consider a  $d$ -dimensional lattice model with lattice constant  $a$  and length  $L$  in each direction. In order to keep the notation simple, we will give the formulae for the case of one dimension, which can be generalized to higher dimensions in a straightforward manner.

A positive definite density in phase space is given by the Husimi function [8] or  $Q$  function [9]

$$\varrho(x_0, k_0) = |\langle x_0, k_0 | \psi \rangle|^2. \quad (1)$$

Here, the state  $|\psi\rangle$  is projected onto a minimal uncertainty state  $|x_0, k_0\rangle$  centered around position  $x_0$  and momentum

<sup>a</sup> e-mail: [ingold@physik.uni-augsburg.de](mailto:ingold@physik.uni-augsburg.de)

<sup>b</sup> UMR 7504 (CNRS-ULP)

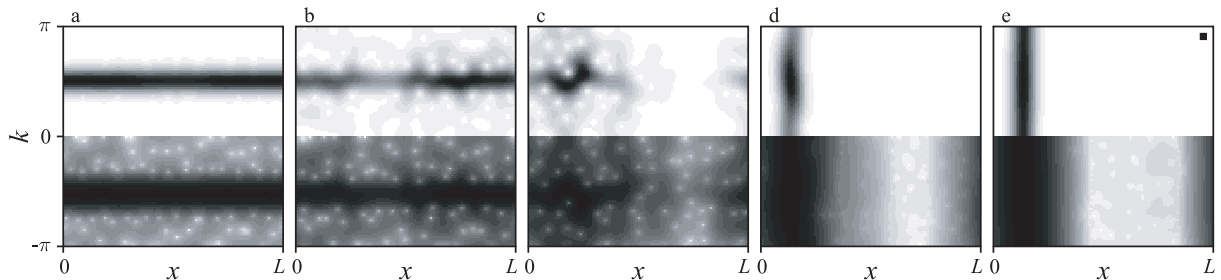


**Fig. 1.** The Husimi function of a state at the band center is shown for a one-dimensional Anderson model of size  $L = 128$  with disorder strengths  $W = 0.1, 1, 2.5, 10,$  and  $25$  increasing from left to right. Exploiting the symmetry with respect to  $k = 0$  the Husimi function is plotted on a linear and logarithmic scale in the upper and lower half, respectively. The gray values from white to black for increasing Husimi function have been normalized separately in each panel. The width  $\sigma$  of the Gaussian (2) is indicated by the black square in panel (e).

$k_0$ . In position representation, the latter assumes a Gaussian form

$$\langle x|x_0, k_0 \rangle = \left( \frac{1}{2\pi\sigma^2} \right)^{1/4} \exp \left( -\frac{(x-x_0)^2}{4\sigma^2} + ik_0x \right) \quad (2)$$

where the value of the variance  $\sigma^2$  is yet undetermined. The Husimi function is normalized,  $\int (dxdk/2\pi)\varrho(x, k) = 1$ , and, for real wave functions  $\psi(x)$ , obeys the symmetry  $\varrho(x_0, k_0) = \varrho(x_0, -k_0)$ .

The variance  $\sigma^2$  of the Gaussian (2) determines the relative importance of real and momentum space. In the following, we choose  $\sigma^2 = La/4\pi$  leading to equal widths of the Gaussian in  $x$ - and  $k$ -direction. In order to obtain sufficient resolution, one has to ensure that  $\sigma \ll L$  which limits the possible system sizes from below. Then, the effect of neglecting the tails of the Gaussian in finite size systems in presence of periodic boundary conditions will also be small. Examples of Husimi functions for one-dimensional disordered systems are presented in Figure 1, which will be discussed in detail below.

For practical purposes a more global description of the phase space properties is appropriate. Based on the Husimi function the so-called Wehrl entropy [10–12] is defined, which represents a measure of the phase space occupation. It was shown for the driven rotor that the Wehrl entropy of individual quantum states is connected to the energy level statistics [13]. A very similar system, the kicked rotor, can be mapped onto the Anderson model [14], suggesting that the Wehrl entropy is a useful quantity for the characterization of the eigenstates of the Anderson model [15].

A more convenient quantity is the inverse participation ratio (IPR) in phase space

$$P = \int \frac{dx dk}{2\pi} [\varrho(x, k)]^2, \quad (3)$$

which has been employed to measure the complexity of quantum states [16]. This IPR corresponds to a linearization of the Wehrl entropy [17] and can be compared directly to the corresponding quantities  $P_x = \int dx |\psi(x)|^4$  and  $P_k = \int dk |\tilde{\psi}(k)|^4$  in real and momentum space, respectively.  $P_x$  is particularly well studied as it is related

to the probability for a diffusing particle to return to its original position in the long-time limit [18].

Furthermore,  $P$  can be evaluated without recourse to the  $2d$ -dimensional Husimi function. In fact, only the wave function is required since we can recast (3) in the form [19]

$$P = \frac{1}{8\sqrt{\pi}\sigma} \int du \left| \int dv \left( \frac{1}{2}(u-v) \right) \left( \frac{1}{2}(u+v) \right) \times \exp \left( -\frac{v^2}{8\sigma^2} \right) \right|^2. \quad (4)$$

Its nondiagonal character provides the information on momentum. It is only by means of (4) that one succeeds in determining the IPR for three-dimensional systems.

In the following, we specifically consider the Anderson model for non-interacting electrons on a lattice with periodic boundary conditions, where disorder is modeled by a random on-site potential. In  $d = 1$ , the Hamiltonian reads

$$H = -t \sum_n (|n\rangle\langle n+1| + |n+1\rangle\langle n|) + W \sum_n v_n |n\rangle\langle n| \quad (5)$$

with Wannier states  $|n\rangle$  localized at sites  $n = 1, \dots, L$ . All lengths are measured in units of the lattice constant  $a = 1$ . The hopping matrix element  $t = 1$  between neighboring sites defines the energy scale. The on-site energies  $v_n$  are drawn independently from a box distribution on the interval  $[-1/2; 1/2]$  and  $W$  denotes the disorder strength.

Husimi functions for a state at the band center are presented in Figure 1 for increasing disorder strength  $W$  and a randomly selected disorder realization  $v_n$ . Making use of the symmetry with respect to  $k = 0$ , the Husimi function is plotted on a linear and logarithmic gray scale in the upper and lower half, respectively. White points in the lower half may be related to the zeros of the Husimi function [20].

For  $W = 0.1$  (Fig. 1a), the disorder represents only a small perturbation and the Husimi function is thus still close to that of plane waves. Except for the states at the band edges, one finds two stripes well localized at the corresponding  $k$ -values, which are extended over the full real space. The width of the stripes is induced by the projection onto the Gaussian (2). In Figure 1e the opposite limit

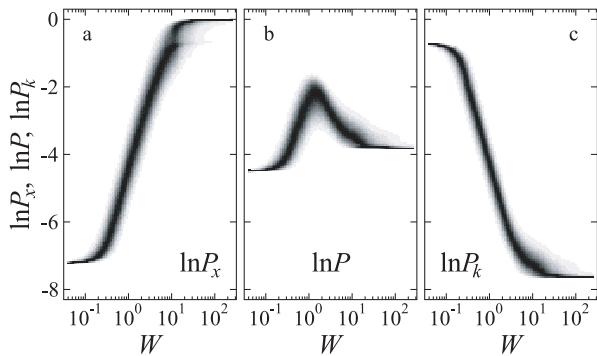


**Fig. 2.** Distributions of the logarithms of the IPR for 50 disorder realizations in (a) real space, (b) phase space, and (c) momentum space as a function of the disorder strength  $W$  for a one-dimensional system of length  $L = 2048$ .

is depicted. At  $W = 25$ , the hopping is a small perturbation,  $t \ll W$ , and the state is localized in real space.

In Figure 1d, where  $W = 10$ , the influence of the nearest neighbor hopping becomes relevant and tends to extend the wave function in real space over several sites. Since the coupled states have to remain orthogonal, they separate in momentum space. This leads to a contraction of the Husimi function in  $k$  direction, which is more important than the spreading over a few sites. As a consequence, the phase space properties for strong disorder are dominated by the behavior in momentum space and the IPR in phase space increases with decreasing disorder. This behavior will also be evident from Figures 2 and 3 below.

Similarly, at weak disorder, the transition from Figure 1a to Figure 1b, *i.e.* to  $W = 1$ , can be understood in terms of a coupling between different plane waves. Here, however, the coupling is not restricted to neighboring  $k$  values, but is governed by the energy difference of the respective states. For one-dimensional systems, the contraction in real space dominates the spreading in momentum space, again leading to an increase of the IPR in phase space (*cf.* Fig. 2b).

As a consequence of the behavior for weak and strong disorder, one expects a maximum for the IPR at intermediate disorder strength. Indeed, for  $W = 2.5$ , the state shown in Figure 1c displays strong localization in phase space.

The situation just described is generic for one-dimensional systems. This can be seen from the distributions of the IPR depicted in Figure 2. The distributions of the logarithms of  $P$  as well as  $P_x$  (real space) and  $P_k$  (momentum space) have been obtained by diagonalizing equation (5) for 50 different disorder realizations  $v_n$  for each disorder strength  $W$  and taking  $L/2$  states around the band center into account.

In the limit of very strong disorder, the states are localized on a single site in real space and uniformly distributed over momentum space. This leads to the limiting values  $P_x(\infty) = 1$  and  $P_k(\infty) = L^{-d}$ . In phase space one has to account for the finite width of the Husimi function and thus finds  $P(\infty) = L^{-d/2}$ . For  $d = 1$ , these values can be checked against the data shown in Figure 2. Starting

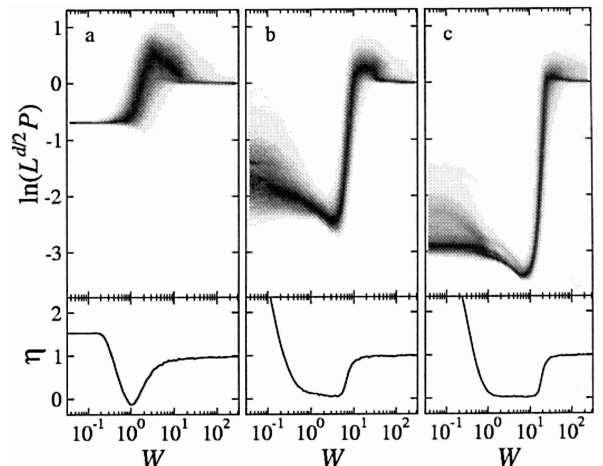


**Fig. 3.** Distributions of the logarithms of the IPR in phase space (top) and  $\eta$  defined in equation (6) (bottom) are shown as a function of disorder strength  $W$  for (a)  $d = 1$ ,  $L = 128$ , (b)  $d = 2$ ,  $L = 64$ , and (c)  $d = 3$ ,  $L = 20$ . The distributions are based on 250, 20, and 20 disorder realizations, respectively.

from this limit, with decreasing disorder two energetically almost degenerate states become coupled *via* the finite hopping matrix element  $t$ . For these states  $P_x$  is reduced to  $1/2$  while  $P_k$  is enhanced by a factor of  $3/2$ . As already discussed above, it is the latter which dominates the behavior in phase space.

In the opposite limit  $W \rightarrow 0$ , the real wave functions in  $d = 1$  contain equal contributions from degenerate plane waves of momenta  $k$  and  $-k$ . This implies  $P_k(0) = 1/2$  and  $P_x(0) = 2/3L$ . In phase space, the finite width of the Husimi function leads to  $P(0) = 1/2L^{1/2}$ . In higher dimensions, however, degeneracies occur and render the behavior for  $W \rightarrow 0$  more complex. Nevertheless, as a function of system size,  $P_x$  and  $P$  scale as  $L^{-d}$  and  $L^{-d/2}$ , respectively. A more detailed discussion will be presented elsewhere [21].

After this comparison of the IPR in different spaces, we now concentrate on the IPR in phase space. The upper part of Figure 3 shows the distributions of the logarithm of  $P$  for dimensions  $d = 1, 2$ , and  $3$  and system sizes  $L = 128, 64$ , and  $20$ , respectively. For better comparison the data have been scaled by the length dependence  $L^{-d/2}$ , being valid in the limits  $W \rightarrow 0$  and  $\infty$ .

The most striking difference between the one-dimensional case and higher dimensions consists in the behavior of the IPR for weak disorder. For  $d = 1$ , the average IPR increases with disorder strength and eventually goes through a maximum. The overall behavior can be understood as a crossover from a regime dominated by real space properties to one dominated by momentum space.

In contrast, in  $d \geq 2$  the average IPR initially decreases. This implies a spreading of the Husimi function beyond the broadened stripes present for weak disorder (*cf.* Fig. 1a). On the other hand, the behavior at strong disorder is governed by the same mechanism as for the one-dimensional case, which implies an increase of the IPR with decreasing disorder. The two regimes are joined by

a short interval of disorder strengths where the Husimi function contracts strongly as disorder is increased.

The main difference of the behavior of  $P$  in  $d \geq 2$  compared to  $d = 1$  consists in the existence of a minimum of  $P$ . This implies a large spread of the eigenstates in phase space indicating the diffusive nature of these states. This interpretation is consistent with the expected absence of diffusion in  $d = 1$  and its appearance in  $d \geq 2$ .

For  $d = 2$  and  $3$ , the distributions of  $P$  depicted in Figures 3b and c behave similarly. However, the pertinent scaling argument for Anderson localization [3] predicts a phase transition only in dimensions higher than two. While in  $d = 3$  a diffusive regime appears even in the thermodynamic limit, in  $d = 2$  it is present for systems of finite size when the system size exceeds the mean free path but not the localization length. Unfortunately, in  $d = 3$ , numerical constraints prevent us from performing a sound finite size scaling, which would allow to distinguish the form of the jumps of  $P$  in  $d = 2$  and  $3$  in the thermodynamic limit  $L \rightarrow \infty$ . Nevertheless, an analysis of the distributions of  $P$  for different system sizes exhibits clear differences between  $d = 2$  and  $3$  [21]. In  $d = 2$ , the minimum together with the jump shifts to smaller disorder strengths with increasing  $L$ . In contrast, for  $d = 3$ , the minimum shifts in the opposite direction and the jump remains at finite disorder strength giving evidence for the Anderson transition at  $W \approx 16.5$ .

To further substantiate our findings about the signatures of the different transport regimes in phase space, we compare our results to energy level statistics. In the diffusive regime the energy spacing distribution  $p(s)$  is close to the Wigner-Dyson distribution  $p_W(s) = \frac{1}{2}\pi s \exp(-\pi s^2/4)$ . In contrast, in the localized regime,  $p(s)$  approaches the Poissonian statistics  $p_P(s) = \exp(-s)$ . To quantify the form of the distribution we evaluate

$$\eta = \frac{\int_0^b ds(p(s) - p_W(s))}{\int_0^b ds(p_P(s) - p_W(s))} \quad (6)$$

which is particularly sensitive to level repulsion. Here,  $b = 0.4729\dots$  refers to the first crossing point of the distributions  $p_W(s)$  and  $p_P(s)$ . According to its definition,  $\eta = 1$  for a Poissonian spacing distribution and  $\eta = 0$  for a Wigner-Dyson spacing distribution.

In the lower part of Figure 3,  $\eta$  is shown as a function of the disorder strength. For weak disorder,  $\eta$  exceeds 1 because of non-universal level statistics appearing in regular geometries in the ballistic regime. For strong disorder one finds Poissonian statistics as expected for the localized regime. At intermediate disorder strengths in  $d = 1$ ,  $\eta$  exhibits a minimum due to level repulsion, but no proper diffusive regime exists. On the other hand, for finite size systems in  $d = 2$ , an extended region is present, where the level statistics is close to that predicted by random matrix theory. This property is commonly used to identify a region of diffusive dynamics. For  $d = 3$  the diffusive region survives even in the thermodynamic limit  $L \rightarrow \infty$ .

Figure 3 clearly shows that the decrease of the IPR is related to a plateau of  $\eta$  at values close to zero. Using the

spreading of the states in phase space as an indicator for diffusive behavior is therefore consistent with the results from level statistics. For  $d = 3$ , a comparison between  $\eta$  and the distribution of  $P$  even allows to identify the ballistic regime for weak disorder, where the IPR essentially remains constant.

In conclusion, we have shown that phase space properties represent a new tool to describe disordered systems for arbitrary disorder strength. The IPR in phase space provides information, which could not be obtained from the corresponding quantities  $P_x$  in real space and  $P_k$  in momentum space. It is only the first quantity which captures the appearance of a diffusive regime in two and higher dimensions. Given our demonstration that the physics in phase space is able to provide new insight into the dynamics of disordered systems, these concepts likely will also make a valuable contribution towards understanding the challenging problem of the combined effects of interaction and disorder in few-body systems.

We acknowledge useful discussions with I. Varga. Financial support was provided by the Deutsche Forschungsgemeinschaft through SFB 484 and the European Union within the RTN program (D.W.). The numerical calculations were carried out partly at the Leibniz-Rechenzentrum München.

## References

1. A. Wax, S. Bali, J.E. Thomas, Phys. Rev. Lett. **85**, 66 (2000).
2. A.D. Mirlin, Phys. Rep. **326**, 259 (2000).
3. E. Abrahams, P.W. Anderson, D.C. Licciardello, T.V. Ramakrishnan, Phys. Rev. Lett. **42**, 673 (1979).
4. P.A. Lee and T.V. Ramakrishnan, Rev. Mod. Phys. **57**, 287 (1985).
5. P. Pradhan, S. Sridhar, Phys. Rev. Lett. **85**, 2360 (2000).
6. P.W. Anderson, Phys. Rev. **109**, 1492 (1958).
7. B. Kramer, A. MacKinnon, Rep. Prog. Phys. **56**, 1469 (1993) and references therein.
8. K. Husimi, Proc. Phys. Math. Soc. Jpn **22**, 264 (1940).
9. K.E. Cahill, R.J. Glauber, Phys. Rev. **177**, 1882 (1969).
10. A. Wehrl, Rep. Math. Phys. **16**, 353 (1979).
11. B. Mirbach, H.J. Korsch, Phys. Rev. Lett. **75**, 362 (1995).
12. S. Gnutzmann, K. Życzkowski, J. Phys. A **34**, 10123 (2001); K. Życzkowski, Physica E **9**, 583 (2001).
13. T. Gorin, H.J. Korsch, B. Mirbach, Chem. Phys. **217**, 145 (1997).
14. S. Fishman, D.R. Grempel, R.E. Prange, Phys. Rev. Lett. **49**, 509 (1982).
15. D. Weinmann, S. Kohler, G.-L. Ingold, P. Hänggi, Ann. Phys. (Leipzig) **8**, SI277 (1999).
16. A. Sugita, H. Aiba, Phys. Rev. E **65**, 036205 (2002); A. Sugita, arXiv preprint, nlin.CD/0112042.
17. There are subtle differences between entropies and inverse participation ratios as was discussed in real space in I. Varga J. Pipek, J. Phys. Cond. Matt. **6**, L115 (1994).
18. D.J. Thouless, Phys. Rep. **13**, 93 (1974).
19. G. Manfredi, M.R. Feix, Phys. Rev. E **62**, 4665 (2000).
20. P. Leboeuf, A. Voros, J. Phys. A **23**, 1765 (1990).
21. A. Wobst, G.-L. Ingold, P. Hänggi, D. Weinmann, unpublished.